DOI: 10.1002/ejic.200801139

Detailed Description of the Metal-to-Ligand Charge-Transfer State in Monoterpyridine Ir^{III} Complexes

Naokazu Yoshikawa,*[a] Shinichi Yamabe,[b] Nobuko Kanehisa,[c] Tsuyoshi Inoue,[c] Hiroshi Takashima,[a] and Keiichi Tsukahara[a]

Keywords: Iridium / N ligands / Charge transfer / Emission / Density functional calculations

We synthesized four Ir^{III} terpyridine complexes with three Cl^- anions by using microwave irradiation. By introducing three Cl^- anions to the Ir^{3+} cation, it can be expected that the absorption and emission properties of the complexes change from π–π* to metal-to-ligand charge transfer (MLCT). These complexes having intrinsic C_{2v} symmetry are suitable for analyzing orbital interactions. This symmetry has four irreducible representations, a_1, a_2, b_1, and b_2, which results in no degenerate orbitals. Charge transfers (CTs) from three nitrogen lone-pair orbitals to the $5d_{z^2}$ and $5d_{x^2-y^2}$ atomic orbitals give three Ir–N coordination bonds in the in-plane molecular orbital (MO) overlap of a_1 symmetry. These CTs are described by the 60th and 66th MOs in the $[IrCl_3(terpy)]$ complex, (terpy = 2,2′:6′,2′′-terpyridine). The antibonding combination of the $5d_{xz}$ and the lone-pair orbital of Cl^- gives rise to the high-lying HOMO in b_1 symmetry. The back CT, the highest occupied molecular orbital (HOMO) (b_1) → the lowest unoccupied molecular orbital (LUMO) (b_1), corresponds to MLCT, and the small-energy excitation is confirmed by the long wavelength $\lambda_{max} \approx 500$ nm in the absorption spectroscopy.

Introduction

In recent years, interest has been devoted to Ir^{III} metal complexes.[1–6] In particular, Ir^{III} cyclometalated complexes have attracted a great deal of attention because of their possible applications as photonic devices[7–10] and organic light-emitting diode displays.[11] The emission color can be tuned from red to blue through ligation of different ancillary ligands or by introducing a variety of donating or accepting groups on the ligands.[12–14] Strong field ligands such as cyanide, carbonyl, and phosphane groups have been introduced in the coordination sphere to increase the energy gap between the highest occupied molecular orbital (HOMO) and the lowest unoccupied molecular orbital (LUMO) and to achieve hypsochromic shift in the emission.[15]

Sauvage et al. reported detailed structural considerations of $[Ir(terpy)_2]^{3+}$ (terpy = 2,2′:6′,2′′-terpyridine).[16] The substitution at the 4′-position of the terpy ligand enables the construction of linearly arranged systems and also has the advantage of avoiding the coexistence of geometrical isomers and stereoisomers. Recently, we focused on Ir^{III} complexes with terpy, 4′-(4-tolyl)-2,2′:6′,2′′-terpyridine (tterpy), and/or polypyridine ligands.[17–19] These iridium(III) complexes have intense phosphorescences at room temperature and remarkably high quantum yields close to unity.[20] In contrast to the experimental studies, however, theoretical efforts on deep understanding phosphorescent emission seem deficient. Only a few excited-state calculations using time dependent density functional theory (TDDFT) on Ir^{III} complexes have been reported.[21–23]

In this work, we have focused on four Ir^{III} terpyridine complexes with three Cl^- anions. These complexes having intrinsic C_{2v} symmetry are suitable for analyzing orbital interactions. This symmetry has four irreducible representations, a_1, a_2, b_1, and b_2, which results in no degenerate orbitals. Then, we performed DFT calculations on the Ir^{III} terpyridine complexes toward better understanding of the absorption and phosphorescent behavior. By analysis of orbital compositions and transition characters of the complexes, we may clarify the interaction between iridium and ligands and improve the optical properties by using appropriate ligands. By introducing three Cl^- anions to the Ir^{3+} cation, it can be expected that the absorption and emission properties of the complexes change from π –π* to metal-to-ligand charge transfer (MLCT).

[a] Department of Chemistry, Faculty of Science, Nara Women's University,
Nara 630-8506, Japan
Fax: +81-742-20-3395
E-mail: naokazuu@dream.com
[b] Department of Chemistry, Nara University of Education, Nara 630-8528, Japan
[c] Department of Applied Chemistry, Graduate School of Engineering, Osaka University, Osaka 565-0871, Japan

Supporting information for this article is available on the WWW under http://www.eurjic.org or from the author.

Results and Discussion

Absorption Properties

Structural formulae of five complexes investigated are shown in Figure 1. Figure 2 shows the absorption spectra for complexes **1**, **2**, and **3**. Absorption data are collected in Table 1. For complex **1**, a strong UV absorption is found in the region 260–330 nm, which is ascribable to intraligand-centered (LC) transitions. At lower energies, less intense absorption spectra are also found at 408 and 523 nm. A slight difference between complex **2** and parent complex **1** is the appearance of a slightly redshifted band centered at 413 and 527 nm for complex **2**, which reflects the effect of the Cl substituent. In each complex, peaks at 413 and 408 nm are assigned to a spin-allowed MO (Ir^{3+} cation and Cl^- anion → terpy) transition. Weak and low-energy band peaks at 523 and 527 nm are assigned to another MO (Ir^{3+} cation and Cl^- anion → terpy) transition. The absorption spectra for complexes **4** and **5** are shown in Figure 3. For complex **4**, weak and low-energy band peaks at 521 nm relative to that of parent complex **1** are not observed. This suggests that complex **4** has a nonplanar structure due to the steric hindrance between the Cl^- anion and the Br substituent. For complex **5**, a redshifted shoulder at around 400 nm in comparison to the band of parent complex **1** is observed. Weak and low-energy band peaks at 521 nm for complex **5** can be assigned to the MO (Ir^{3+} cation and Cl^- anion → tterpy) transition.

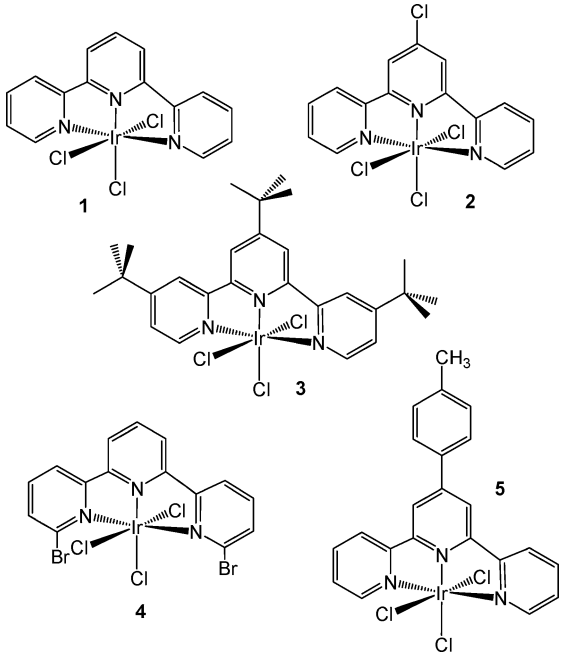

Figure 1. Structures of $[IrCl_3(L)]$.

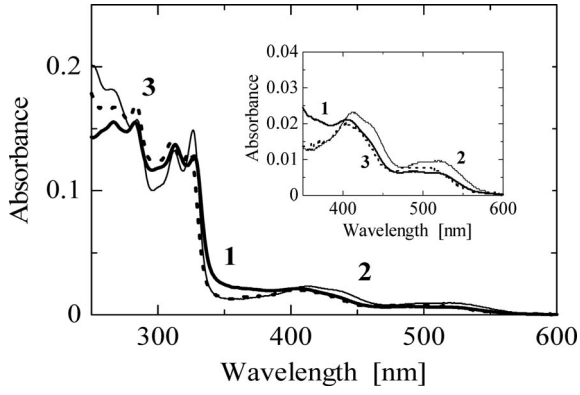

Figure 2. UV/Vis spectra of the iridium complexes: $[IrCl_3(terpy)]$ (**1**; bold line), $[IrCl_3(Clterpy)]$ (**2**; solid line), and $[IrCl_3(Bterpy)]$ (**3**; bold dotted line) in CH_3CN solution (1.0×10^{-5} M) at 25 °C. In the inset, the region of absorbance is expanded.

Table 1. Absorption, emission, and electrochemical properties of the iridium terpyridine complexes in CH_3CN at 25 °C.

Complexes	λ [nm]						λ_{em} [nm]	τ [μs]	Φ[a]	E_{pc} [V]	E_{po} [V]	ΔE [V]
	π–π*				MLCT							
$[IrCl_3(terpy)]$ (**1**)	266	282	313	327	408	523	584 (327)[b]	0.29	0.075	–1.1	1.69	2.79
					400 (0.004)[c]	527 (0.027)[c]	580 (0.024)[c]					(2.71)[d]
$[IrCl_3(Clterpy)]$ (**2**)	265	283	312	327	413	527	600 (327)[b]	0.43	0.094	–1.04	1.68	2.73
					416 (0.004)[c]	545 (0.023)[c]	604 (0.026)[c]					(2.67)[d]
$[IrCl_3(Bterpy)]$ (**3**)	269	283	310	324	405	514	591 (324)[b]	0.49	0.0069	–1.18	1.59	2.77
						516 (0.024)[c]	578 (0.018)[c]					(2.77)[d]
$[IrCl_3(Brterpy)]$ (**4**)		293	327	340	419		567 (327)[b]	0.5	0.019			
					440 (0.012)[c]		619 (0.018)[c]					(2.39)[d]
$[IrCl_3(tterpy)]$ (**5**)		328	348	373		521	591 (328)[b]	0.66	0.0071	–1.09	1.64	2.73
						523 (0.025)[c]	601 (0.032)[c]					(2.68)[d]
$[Ir(terpy)_2](PF_6)_3$[e]	251	277	313	325	352		458	1.2	0.025			
$[Ir(tterpy)_2](PF_6)_3$[e]	251	278	306	346	374		506	2.4	0.029			

[a] The emission quantum yields were determined at room temperature relative to those of a solution containing $[Ru(bpy)_3]^{2+}$ (Φ = 0.062) and having the same absorbance. [b] Values in parentheses are the excitation wavelengths. [c] From DFT. Values in parentheses are the oscillator strengths. [d] From DFT. [e] From ref.[16]

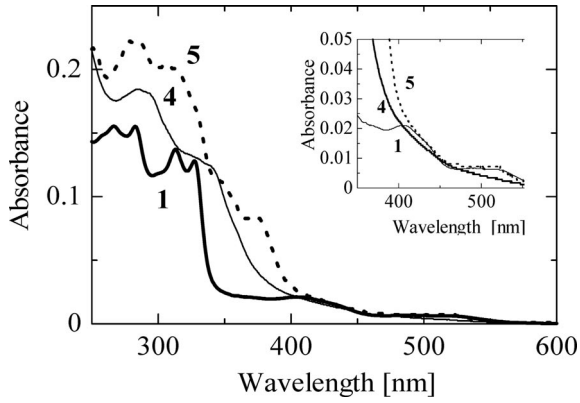

Figure 3. UV/Vis spectra of the iridium complexes: [$IrCl_3$(terpy)] (**1**; bold line), [$IrCl_3$(Brterpy)] (**4**; solid line), and [$IrCl_3$(tterpy)] (**5**; bold dotted line) in CH_3CN solution (1.0×10^{-5} M) at 25 °C. In the inset, the region of absorbance is expanded.

Electrochemistry

The electrochemical properties of the monoterpyridine complexes were examined by cyclic voltammetry in CH_3CN at room temperature (Figure 4). The redox potentials measured relative to Ag/AgCl are summarized in Table 1. For complex **1**, a reversible one-electron oxidation wave was observed at 1.69 V. In general, the Ir^{IV}/Ir^{III} redox couple in iridium(III) complexes with terpyridine ligands cannot be observed in a conventional potential window.[24] This low oxidation potential value reflects the increase in the electronic density at the Ir center. A reversible one-electron oxidation wave was also observed for the other iridium complexes at around 1.69 V. Several reports in the literatures indicate that these processes are due to the removal of the metal-localized electron.[24,25] At negative potentials, complex **2** exhibits a reversible one-electron process at –1.04 V. A similar pattern is observed for complex **3** at –1.18 V. By comparison with the related complexes, these processes can be assigned to the reduction of the terpyridine ligand. The LUMO may be the π* orbital on the terpy derivatives.

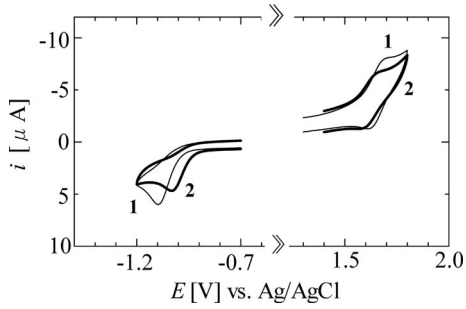

Figure 4. CV of the iridium complexes: [$IrCl_3$(terpy)] (**1**; solid line) and [$IrCl_3$(Clterpy)] (**2**; bold solid line) in CH_3CN solution (5.0×10^{-4} M) at 25 °C with a scan rate of 100 mV s^{-1}.

Emissions Properties

The new complexes are luminescent in solution at room temperature and display a single structureless emission band, typical of phosphorescence from the excited states of CT character. The emission spectrum of parent complex **1** at 584 nm (excitation wavelength 327 nm) is shown in Figure 5. The lifetime of complex **1** was measured in CH_3CN at room temperature. The relatively long lifetime (0.29 μs) of complex **1** was obtained. Other complexes have similar lifetimes, which indicate the emissions of these complexes should be MLCT phosphorescence. The redshift at 600 nm in complex **2** and the slight redshift at 591 nm in complex **3** in the emission maxima were observed. The two Br substituents in complex **4** have an influence on the emission maximum. This complex, having a nonplanar structure and some electronic effects consequent to the positioning of the Br centers that are opposite to the direction of the MLCT transition, indicates blueshift at 567 nm. In contrast, the tolyl substitution for complex **5** shows a redshift in the emission maximum at 591 nm. A linear correlation was observed between the energy of the CT excited state and the difference between the ground-state first oxidation and first reduction potentials (Table 1).

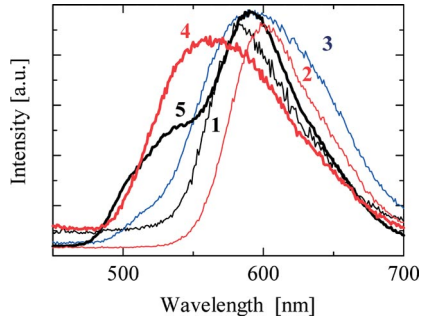

Figure 5. Emission spectra of the iridium complexes in CH_3CN solution at 25 °C: [$IrCl_3$(terpy)] (**1**; λ_{ex} = 327 nm; solid line), [$IrCl_3$(Clterpy)] (**2**; λ_{ex} = 327 nm; red line), [$IrCl_3$(Bterpy)] (**3**; λ_{ex} = 324 nm; blue line), [$IrCl_3$(Brterpy)] (**4**; λ_{ex} = 327 nm; bold red line), and [$IrCl_3$(tterpy)] (**5**; λ_{ex} = 328 nm; bold line).

Computational Results

Structures of Complexes 1–5

Geometries optimized by using RB3LYP/LANL2DZ[6-311+G(d)] for the ground state of the complexes are shown in Figure 6. Further geometrical parameters are collected in Table S1 (Supporting Information). Complexes **1** and **2** have the C_{2v} point group with the central nitrogen atom, Ir^{3+}, and one ligand Cl^- anion oriented along the principal *z* axis. The terpyridine ring is located in the *yz* plane. The optimized structures of complexes **1** and **2** (and practically complex **3**) are of C_{2v} symmetry, where the NCCN dihedral angle is 0°. However, the dihedral angles N1–C–C–N2 and N2–C–C–N3 in complex **4** are 9.05 and 9.19°, respectively,

owing to the steric crowd by the bulky Br substituents. In complex **5**, the dihedral angle N–C–C–N of the terpy ligand is 0.29°. In contrast, the dihedral angle between the tolyl substituent and the central pyridine is 40.47°.

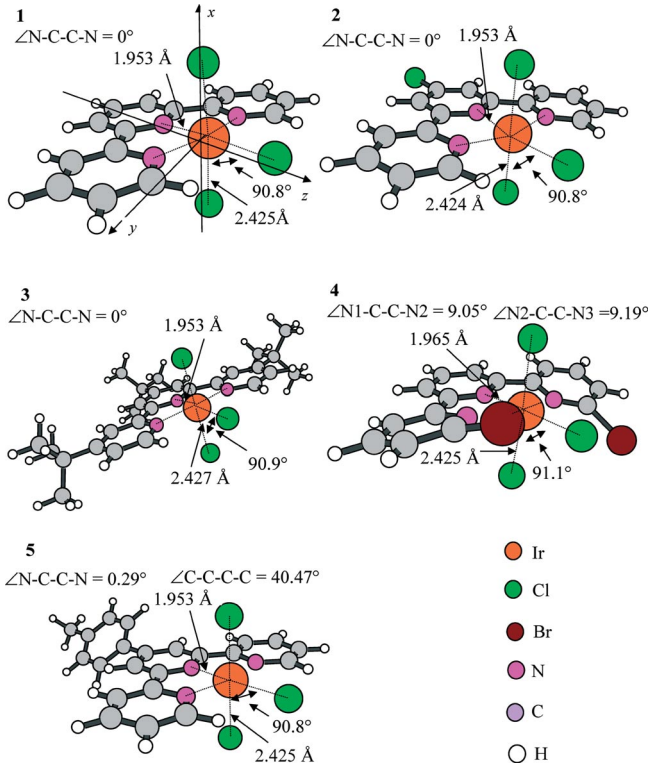

Figure 6. Optimized geometries calculated by using RB3LYP/LANL2DZ[6-311+G(d)] for the ground state of complexes **1**–**5**. Dihedral angles are also shown.

Orbital Interactions in Complexes 1 and 4

The Ir^{3+} cation has $5d^6$ electronic configuration and a quintet spin state (four parallel spins) according to Hund's rule. When the cation is surrounded by ligands, a singlet spin state is brought about by promotion. Two vacant atomic orbitals, $5d_{z^2}$ and $5d_{x^2-y^2}$, belong to the a_1 symmetry and are found to be fit for the in-phase [Scheme 1 (1–1)] and antiphase [Scheme 1 (1–2)] orbital overlaps, respectively. In the (1–1) phase, the white lobe of the $5d_{z^2}$ orbital is subject to the charge flow from lone-pair orbitals of the central nitrogen atom and a chloride ion along the *z* axis. The shaded lobe of the $5d_{z^2}$ orbital is connected to the two lone-pair orbitals along the *y* axis. In the (1–2) phase, the shaded lobe is subject to the charge flow from two lone-pair orbitals along the *y* axis. The white lobe overlaps with the Cl^- lone-pair orbitals along the *x* axis. Thus, the $N \rightarrow Ir^{3+}$ σ-type coordination bonds (i.e., charge transfer) are established within the a_1 symmetry. The (1–1) and (1–2) modes are expressed by the 60th and 66th occupied MOs, respectively. Then, back CT should occur within a_2, b_1 and/or b_2 symmetries.

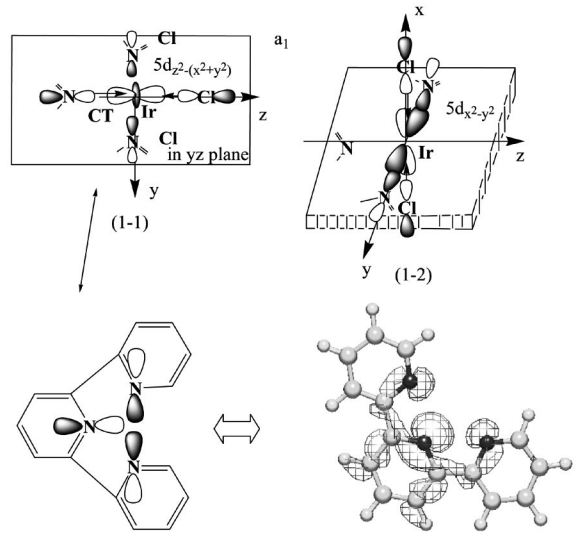

Scheme 1. Charge transfer interactions that give three Ir–N covalent bonds.

The three Ir^{3+} lone-pair orbitals $5d_{xy}$, $5d_{yz}$, and $5d_{xz}$ belong to a_2, b_2, and b_1 irreducible representations, respectively. Noteworthy is that each lone-pair orbital mixes with that of the chloride ion in the *xy*, *xz*, or *yz* plane. Obviously, the energy level of Cl^- (anion) is higher than that of Ir^{3+}(cation), and the orbital mixing pattern may be depicted [Scheme 2 (2–1)]. In fact, the calculated MO coefficients of HOMO, HOMO-1, and HOMO-2 in Scheme 2 (2–2) follow the pattern and involve the out-of-plane overlap. This overlap enhances the donor ability of $[IrCl_3(terpy)]$ and consequently the excitation at longer wavelength.

Scheme 3 shows frontier vacant orbitals, where coefficients on the nitrogen atoms correspond to those of Scheme 1 (1–1) and (1–2) in the a_1 symmetry. The LUMO is a typical π* orbital of the conjugate terpy ring. The result suggested by CV data (Figure 4) is confirmed. Complex **2** with a Cl substituent exhibits a reversible one-electron process at –1.04 V. In contrast, complex **3** with a *tert*-butyl substituent shows a reversible one-electron process at –1.18 V. Now, the long wavelength of **1** shown in Figures 2 and 3 is explicable in terms of the symmetry-allowed HOMO(b_1) →LUMO(b_1) excitation. The HOMO level becomes high owing to the antiphase overlap in Scheme 2 (2–1). The LUMO level is low as a result of terpy ring conjugation. The MLCT contains a large component of the lone-pair orbital of the anion (Cl^-) ligands.

Complex **4** does not have C_{2v} symmetry due to the steric crowd of two Br substituents. The symmetry lowering ($C_{2v} \rightarrow C_2$) makes the mixing of (a_1, a_2) → a and (b_1, b_2) → b and consequently gives a new mixing of Scheme 2 (2–1). A reorganization of occupied and vacant orbitals takes place, which leads to the appearance of occupied orbitals of higher energy levels and vacant ones or lower ones. The reorganization is verified by the smaller (HOMO→LUMO) energy gap of **4** than those of **1**, **2**, **3**, and **5** in Figure S1 (Supporting Information). Accordingly, the wavelength 419 nm of **4** is larger than 408 nm of **1** in Table 1.

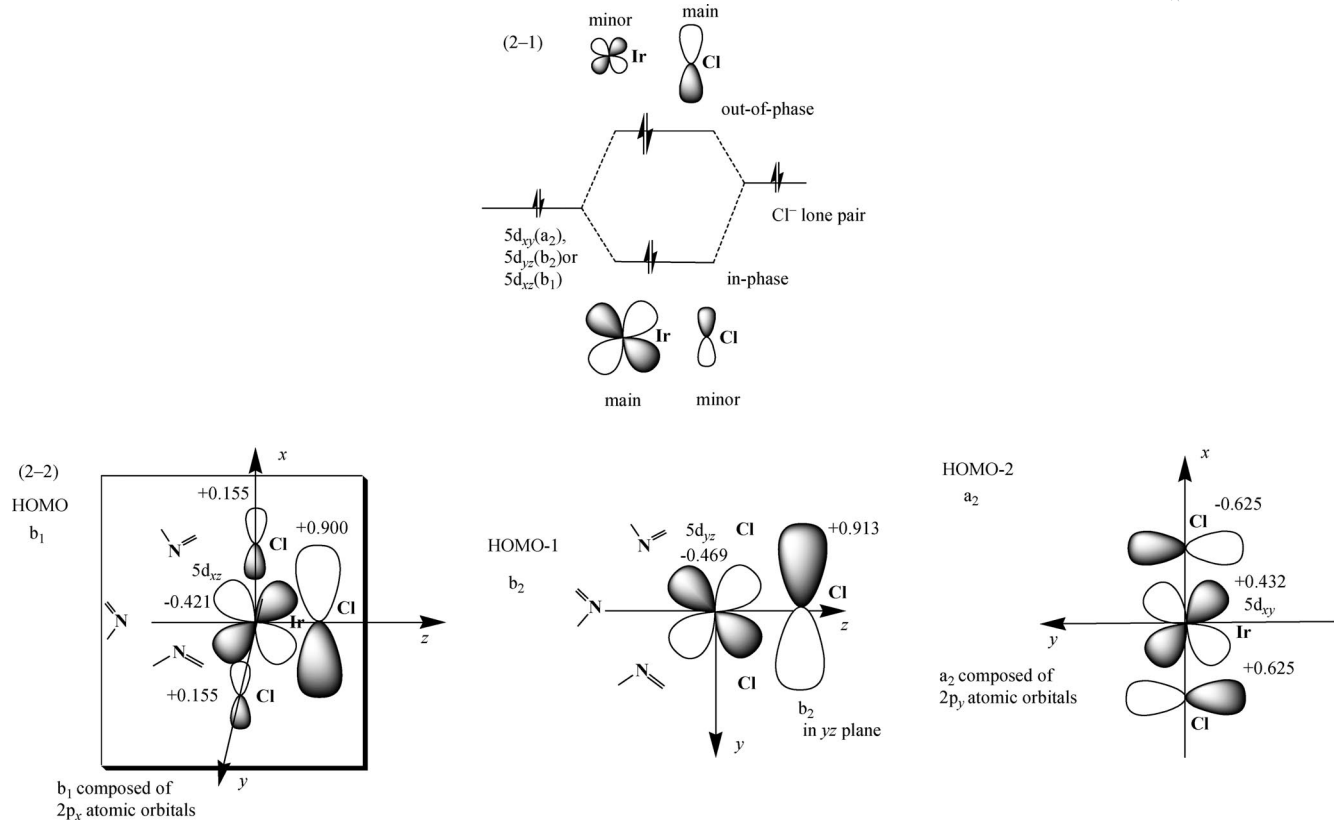

Scheme 2. The fundamental orbital mixing pattern (2–1) and three high-lying occupied MOs of **1** (2–2).

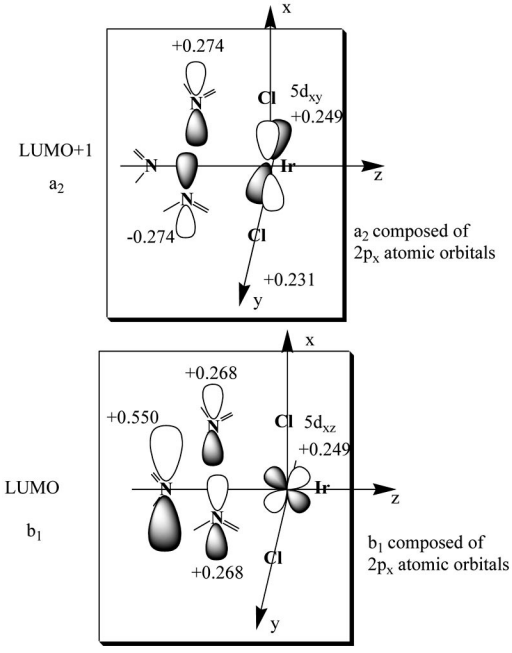

Scheme 3. Two low-lying unoccupied MOs of $[IrCl_3(terpy)]$ (**1**).

Conclusions

We have synthesized four Ir^{III} terpyridine complexes with three Cl^- anions by using microwave irradiation. These complexes having intrinsic C_{2v} symmetry are suitable for analyzing orbital interactions. By introducing three Cl^- anions to the Ir^{3+} cation, it can be expected that the absorption and emission properties of the complexes change from π–π* to MLCT. This symmetry has four irreducible representations, a_1, a_2, b_1, and b_2, which results in no degenerate orbitals. DFT calculations were carried out to determine the structures of the five complexes. The C_{2v} symmetry was confirmed for complexes **1** and **2**, and the others have similar symmetry. All Cl–Ir–Cl angles are almost 90°, which indicates that the direction of 5d orbitals is strictly obeyed in the Ir–Cl coordination. Two charge transfers (CTs) [nitrogen lone-pair orbitals → $5d_{z^2}$ and $5d_{x^2-y^2}$ of Ir^{3+}] gives three N–Ir σ-type coordination bands in the a_1 symmetry. The three lone-pair orbitals $5d_{xy}$, $5d_{yz}$ and $5d_{xz}$ mix strongly with Cl^- ions in the a_2, b_2, and b_1 symmetry, respectively. Their out-of-phase combinations lead to HOMO-2, HOMO-1, and HOMO. The MLCT observed in Figures 2 and 3 is brought about by the high-lying HOMO (out-of-phase) → the low-lying LUMO (π* of the terpy ring conjugation). The lone-pair Cl^- has an indispensable role on MLCT.

Experimental Section

Reagents: The materials used in the present experiments were of analytical grade. The reagents are as follows: ammonium hexachloroiridate {$(NH_4)_3[IrCl_6]$, Aldrich}, terpy (Aldrich), Clterpy = 4′-Chloro-2,2′:6′,2′′-terpyridine, and Bterpy = 4,4′,4′′-tri-(*tert*-butyl)-2,2′:6′,2′′-terpyridine, (Aldrich), Brterpy = 6,6′-dibromo-

2,2′:6′,2′′-terpyridine (Aldrich), tterpy (Aldrich), and potassium hexafluorophosphate (KPF_6, Wako). The complex $[IrCl_3(terpy)]$ (**1**) was synthesized. Tetrabutylammonium perchlorate {TBAP, $[(C_4H_9)_4N]ClO_4$, Aldrich} as a supporting electrolyte was purchased and used without further purification. CH_3CN and *N*,*N*-dimethylformamide (DMF) used in spectroscopic and electrochemical studies were of spectroscopic grade obtained from Dojindo Laboratory. All other reagents and solvents were of guaranteed grade.

Synthesis: The complexes $[IrCl_3(L)]$ (L = terpyridine derivatives) were prepared by a sequential procedure with a ligand replacement. $(NH_4)_3[IrCl_6]$ (0.24 g, 0.50 mmol) and ligand L (0.50 mmol) were mixed in ethylene glycol (15 mL). The suspended mixture was heated at reflux for 15 min in a microwave oven with purging of nitrogen atmosphere. After the mixture was cooled to room temperature, an orange yellow product began to precipitate and was collected by vacuum filtration. The residue was dissolved in a minimal amount of CH_3CN.

Measurements: Electronic absorption spectra were recorded at room temperature in CH_3CN solution with a Shimadzu UV-2550 spectrophotometer. Mass spectra (ESI) were obtained by a JEOL JMS-T100LC AccuTOF spectrometer. All NMR spectra were recorded with a JEOL JNM-AL400 FT-NMR spectrometer. ^1H NMR chemical shift values are reported in ppm as reference to the internal standard TMS. CV were measured with an ALS-610B electrochemical analyzer fitted with a three-electrode system consisting of a glassy carbon working electrode, a platinum auxiliary electrode, and a Ag/AgCl reference electrode. CV experiments were performed for DMF solution of the complexes (5.0×10^{-4} M) and 0.050 M TBAP under a nitrogen atmosphere at 25 °C with a scan rate of 100 mV s^{-1}. The emission lifetimes were measured in nitrogen-equilibrated CH_3CN solutions by using a Horiba single-photon counting system (NAES-500). The emission quantum yields for the iridium complexes were determined in CH_3CN at room temperature relative to those of a solution containing $[Ru(bpy)_3]Cl_2$ and having the same absorbance. The emission quantum yields for the iridium complexes were determined by comparing the integrated emission spectra and by using $\phi = 0.062$ for the standard.[26]

$[IrCl_3(Clterpy)]$(2): Yield: 40% (113 mg). $C_{15}H_{10}Cl_4IrN_3$ (566.30): calcd. C 31.81, H 1.77, N 7.42; found C 31.31, H 2.02, N 7.49. MS (ESI): *m*/*z* = 571.09 $[IrCl_2(Clterpy) + CH_3CN]^+$, 530.05 $[IrCl_2(Clterpy)]^+$. ^1H NMR (400 MHz, CD_3CN): δ = 8.82 (dd, *J* = 5.6 Hz, 2 H), 9.12 (dd, *J* = 8.0 Hz, 2 H), 9.32 (d, *J* = 8.0 Hz, 2 H), 9.46 (s, 2 H), 10.28 (d, *J* = 5.6 Hz, 2 H) ppm.

$[IrCl_3(Bterpy)]$(3): Yield: 30% (105 mg). $C_{27}H_{35}Cl_3IrN_3$ (700.18): calcd. C 46.32, H 5.00, N 6.00; found C 45.81, H 4.88, N 5.88. MS (ESI): *m*/*z* = 705.33 $[IrCl_2(Bterpy) + CH_3CN]^+$, 664.30 $[IrCl_2(Bterpy)]^+$. ^1H NMR (400 MHz, CD_3CN): δ = 1.55 (s, 27 H), 7.79 (d, *J* = 6.0 Hz, 2 H), 8.36 (s, 2 H), 8.37 (s, 2 H), 9.13 (d, *J* = 6.0 Hz, 2 H) ppm.

$[IrCl_3(Brterpy)]$(4): Yield: 25% (86.2 mg). $C_{16}H_{12}Br_2Cl_3IrN_3O$ (689.66): calcd. C 26.67, H 1.99, N 5.83; found C 26.37, H 2.05, N 6.20. MS (ESI): *m*/*z* = 699.92 $[IrCl(Brterpy) + 2CH_3CN]^+$, 617.86 $[IrCl(Brterpy)]^+$.

$[IrCl_3(tterpy)]$(5): Yield: 15% (46.6 mg). $C_{22}H_{17}Cl_3IrN_3$ (621.98): calcd. C 42.48, H 2.75, N 6.76; found C 42.79, H 3.00, N 6.98. MS (ESI): *m*/*z* = 627.18 $[IrCl_2(tterpy) + CH_3CN]^+$, 586.15 $[IrCl_2(tterpy)]^+$. ^1H NMR (400 MHz, CD_3CN): δ = 2.57 (s, 3 H), 7.56 (d, *J* = 8.0 Hz, 2 H), 7.90 (dd, *J* = 6.0 Hz, 2 H), 7.98 (d, *J* = 8.4 Hz, 2 H), 8.22 (dd, *J* = 7.2 Hz, 2 H), 8.56 (d, *J* = 8.8 Hz, 2 H) 8.68 (s, 2 H), 9.40 (d, *J* = 6.0 Hz, 2 H) ppm.

Computational Methods: DFT calculations of complexes **1**–**5** were performed by using the Gaussian98 program package.[27] The Becke three parameters hybrid exchange and the Lee–Yang–Parr correlation functionals (B3LYP) were used.[28,29] Geometries in the ground state were optimized by the RB3LYP/LANL2DZ method.[30] In the basis set LANL2DZ[6-311 + G(d)], LANL2DZ was used for the Ir^{III} metal and 6-311+G(d).[31] was used for other atoms. After the RB3LYP/LANL2DZ[6-311+G(d)] geometry optimizations were completed, single-point calculations of RB3LYP/LANL2DZ [6-311+G(d)] TD SCRF = PCM were carried out for complexes **1**–**5**. The solvent effect of CH_3CN was included by the SCRF = PCM method.[32–37]

Supporting Information (see footnote on the first page of this article): Schematic drawing of the orbital energies of the HOMO and LUMO obtained from B3LYP calculations; calculated bond lengths and angles for the ground states of complexes **1**–**5**; computed TDDFT vertical excitation energies for the lowest singlet excited states of complexes.

[1] I. M. Dixon, J.-P. Collin, J.-P. Sauvage, L. Flamigni, S. Encinas, F. Barigelletti, *Chem. Soc. Rev.* **2000**, *29*, 385–391.
[2] E. Baranoff, J.-P. Collin, J.-P. Sauvage, L. Flamigni, *Chem. Soc. Rev.* **2004**, *33*, 147–155.
[3] L. Flamigni, B. Ventura, F. Barigelletti, E. Baranoff, J.-P. Collin, J.-P. Sauvage, *Eur. J. Inorg. Chem.* **2005**, 1312–1318.
[4] L. Flamigni, A. Barbieri, C. Sabatini, B. Ventura, F. Barigelletti, *Top. Curr. Chem.* **2007**, *281*, 143–203.
[5] P. T. Chou, Y. Chi, *Chem. Eur. J.* **2007**, *13*, 380–395.
[6] F. M. Hwang, H. Y. Chen, P. S. Chen, C. S. Liu, Y. Chi, C. F. Shu, F. L. Wu, P. T. Chou, S. M. Peng, G. H. Lee, *Inorg. Chem.* **2005**, *44*, 1344–1353.
[7] S. Lamansky, P. Djurovich, D. Murphy, F. Abdel-Razzaq, R. Kwong, I. Tsyba, M. Bortz, B. Mui, R. Bau, M. E. Thompson, *Inorg. Chem.* **2001**, *40*, 1704–1711.
[8] S. Lamansky, P. Djurovich, D. Murphy, F. Abdel-Razzaq, H.-E. Lee, C. Adachi, P. E. Burrows, S. R. Forrest, M. E. Thompson, *J. Am. Chem. Soc.* **2001**, *123*, 4304–4312.
[9] A. J. Wilkinson, A. E. Goeta, C. E. Foster, J. A. G. Williams, *Inorg. Chem.* **2004**, *43*, 6513–6515.
[10] K. Dedeian, J. Shi, N. Shepherd, E. Forsythe, D. C. Morton, *Inorg. Chem.* **2005**, *44*, 4445–4447.
[11] S.-B. Zhao, T. McCormick, S. Wang, *Inorg. Chem.* **2007**, *46*, 10965–10967.
[12] Y. You, S. Y. Park, *J. Am. Chem. Soc.* **2005**, *127*, 12438–12439.
[13] J. Li, P. I. Djurovich, B. D. Alleyne, M. Yousufuddin, N. N. Ho, J. C. Thomas, J. Peters, R. Bau, M. E. Thompson, *Inorg. Chem.* **2005**, *44*, 1713–1727.
[14] S.-Y. Takizawa, J.-I. Nishida, T. Tsuzuki, S. Tokito, Y. Yamashita, *Inorg. Chem.* **2007**, *46*, 4308–4319.
[15] Y.-Y. Lyu, Y. Byun, O. Kwon, E. Han, W. S. Jeon, R. R. Das, K. Char, *J. Phys. Chem. B* **2006**, *110*, 10303–10314.
[16] J.-P. Collin, I. M. Dixon, J.-P. Sauvage, J. A. G. Williams, F. Barigelletti, L. Flamigni, *J. Am. Chem. Soc.* **1999**, *121*, 5009–5016.
[17] N. Yoshikawa, T. Matsumura-Inoue, *Anal. Sci.* **2003**, *19*, 761–765.
[18] N. Yoshikawa, J. Sakamoto, N. Kanehisa, Y. Kai, T. Matsumura-Inoue, H. Takashima, K. Tsukahara, *Acta Crystallogr., Sect. E* **2003**, *59*, m830–m832.
[19] N. Yoshikawa, S. Yamabe, N. Kanehisa, Y. Kai, H. Takashima, K. Tsukahara, *Eur. J. Inorg. Chem.* **2007**, 1911–1919.
[20] T. Yutaka, S. Obara, S. Ogawa, K. Nozaki, N. Ikeda, T. Ohno, Y. Ishii, K. Sakai, M. Haga, *Inorg. Chem.* **2005**, *44*, 4737–4746.
[21] P. J. Hay, *J. Phys. Chem. A* **2002**, *106*, 1634–1641.
[22] C. Yang, S. Li, Y. Chi, Y. Cheng, Y. Yeh, P. Chou, G. Lee, C. Wang, C. Shu, *Inorg. Chem.* **2005**, *44*, 7770–7780.
[23] N. Yoshikawa, S. Yamabe, N. Kanehisa, Y. Kai, H. Takashima, K. Tsukahara, *Inorg. Chim. Acta* **2006**, *359*, 4585–4593.

[24] A. Mamo, I. Stefio, M. F. Parisi, A. Credi, M. Venturi, C. Di Pietro, S. Campagna, *Inorg. Chem.* **1997**, *36*, 5947–5950.
[25] A. Auffrant, A. Barbieri, F. Barigelletti, J.-P. Collin, L. Flamigni, C. Sabatini, J.-P. Sauvage, *Inorg. Chem.* **2006**, *45*, 10990–10997.
[26] J. V. Casper, T. J. Meyer, *Inorg. Chem.* **1983**, *22*, 2444–2453.
[27] M. J. Frisch, G. W. Trucks, H. B. Schlegel, G. E. Scuseria, M. A. Robb, J. R. Cheeseman, V. G. Zakrzewski, J. A. Montgomery Jr, R. E. Stratmann, J. C. Burant, S. Dapprich, J. M. Millam, A. D. Daniels, K. N. Kudin, M. C. Strain, O. Farkas, J. Tomasi, V. Barone, M. Cossi, R. Cammi, B. Mennucci, C. Pomelli, C. Adamo, S. Clifford, J. Ochterski, G. A. Petersson, P. Y. Ayala, Q. Cui, K. Morokuma, D. K. Malick, A. D. Rabuck, K. Raghavachari, J. B. Foresman, J. Cioslowski, J. V. Ortiz, A. G. Baboul, B. B. Stefanov, G. Liu, A. Liashenko, P. Piskorz, I. Komaromi, R. Gomperts, R. L. Martin, D. J. Fox, T. Keith, M. A. Al-Laham, C. Y. Peng, A. Nanayakkara, C. Gonzalez, M. Challacombe, P. M. W. Gill, B. Johnson, W. Chen, M. W. Wong, J. L. Andres, C. Gonzalez, M. Head-Gordon, E. S. Replogle, J. A. Pople, *Gaussian 98*, revision A.7, Gaussian Inc., Pittsburgh, PA, USA, **1998**.
[28] C. Lee, W. Yang, R. G. Parr, *Phys. Rev. B* **1988**, *37*, 785–789.
[29] A. D. Becke, *J. Chem. Phys.* **1993**, *98*, 5648–5652.
[30] J. Hay, W. R. Wadt, *J. Chem. Phys.* **1985**, *82*, 299–310.
[31] M. M. Francl, W. J. Petro, W. J. Hehre, J. S. Binkley, M. H. Gordon, D. J. Defree, J. A. Pople, *J. Chem. Phys.* **1982**, *77*, 3654–3665.
[32] B. Mennucci, J. Tomasi, *J. Chem. Phys.* **1997**, *106*, 5151–5158.
[33] M. T. Cances, B. Mennucci, J. Tomasi, *J. Chem. Phys.* **1997**, *107*, 3032–3041.
[34] V. Barone, M. Cossi, J. Tomasi, *J. Chem. Phys.* **1997**, *107*, 3210–3221.
[35] M. Cossi, V. Barone, B. Mennucci, J. Tomasi, *Chem. Phys. Lett.* **1998**, *286*, 253–260.
[36] V. Barone, M. Cossi, J. Tomasi, *J. Comput. Chem.* **1998**, *19*, 404–417.
[37] V. Barone, M. Cossi, *J. Phys. Chem. A* **1998**, *102*, 1995–2001.

Received: November 22, 2008
Published Online: April 1, 2009

